

UNCLASSIFIED

Copy 6
RM E54K30

NACA RM E54K30



RESEARCH MEMORANDUM

NOTE ON THE SCAVENGE OF 6-INCH-DIAMETER RAM-JET
EXHAUST IN MACH 3.1, 1- BY 1-FOOT
SUPERSONIC TUNNEL

By Warren C. Burgess, Jr., and L. Eugene Baughman

Lewis Flight Propulsion Laboratory
Cleveland, Ohio

CLASSIFICATION CHANGED

UNCLASSIFIED

To _____

By authority of *NASA P.A. 3* Date *12-2-58*
NS 2-13-59

CLASSIFIED DOCUMENT

This material contains information affecting the National Defense of the United States within the meaning of the espionage laws, Title 18, U.S.C., Secs. 793 and 794, the transmission or revelation of which in any manner to an unauthorized person is prohibited by law.

NATIONAL ADVISORY COMMITTEE FOR AERONAUTICS

WASHINGTON
February 18, 1955

UNCLASSIFIED

NATIONAL ADVISORY COMMITTEE FOR AERONAUTICS

RESEARCH MEMORANDUM

NOTE ON THE SCAVENGE OF 6-INCH-DIAMETER RAM-JET EXHAUST

IN MACH 3.1, 1- BY 1-FOOT SUPERSONIC TUNNEL

By Warren C. Burgess, Jr., and L. Eugene Baughman

SUMMARY

The exhaust of a 6-inch-diameter ram-jet engine mounted in the Lewis 1- by 1-foot, Mach 3.1 supersonic tunnel was scavenged successfully with a 6.6-inch-diameter scoop. Limiting values of exhaust-to-stream static-pressure ratios and scavenge-system total-pressure ratios were determined for complete scavenging of the products of combustion. The scavenge-system operation influenced the engine exhaust-nozzle pressures under conditions of unstable scavenge flow.

INTRODUCTION

Aircraft power-plant combustion research in return-type supersonic tunnels requires consideration of exhaust scavenging to avoid contamination of the tunnel air by the by-products of combustion. Presented herein are the results of a scavenge study made at the Lewis laboratory in 1952. Although the data pertain to a unique system, their publication is stimulated by the continued interest in the scavenging problem and the absence of published data related thereto.

The influence of the ram-jet fuel-air ratio and the exhaust-nozzle configuration upon the ability of the system to scavenge effectively were determined, and the effect of the proximity of the scavenge system on the engine operation was evaluated. Total pressures indicating the power required for tunnel and scavenge-system operation were also measured.

No attempt was made to improve the system performance by varying the scavenge configuration.

[REDACTED]

SYMBOLS

The following symbols are used in this report:

- D body diameter at nozzle exit (station 2), in.
f/a fuel-air ratio
M Mach number
P total pressure
 p_e static pressure at nozzle exit (station 2)
 p_s stream static pressure at nozzle exit (station 2)
q dynamic pressure, $\frac{1}{2} \rho V^2$
r body radius at nozzle exit (station 2), in.
T total temperature, °R
x distance downstream of nozzle exit
y radial distance measured from the nozzle axis
 τ engine temperature-rise ratio, T_2/T_0

Subscripts:

- 0 stagnation
1 free-stream station ahead of model
2 nozzle exit
3 scavenge scoop inlet
4 scavenge system discharge
5 tunnel diffuser discharge

APPARATUS AND PROCEDURE

The Lewis 1- by 1-foot, Mach 3.1 nonreturn tunnel was used for the scavenge investigation. Inlet air was supplied to the tunnel bellmouth at approximately 50 pounds per square inch absolute pressure, 50° F temperature, and 2.2×10^{-5} specific humidity.

The engine and scavenge-system installations are presented in figure 1. A partially exploded view of the engine is presented in figure 2. The ram-jet engine was 6 inches in diameter, 60 inches in length, and was equipped with a 30° half-angle single cone inlet. The internal geometry consisted of a subsonic diffuser, a combination spray bar and impinging-jet fuel system, a can-type baffle, a length of combustion chamber, and a convergent-divergent exhaust nozzle. Two convergent-divergent exhaust nozzles with design Mach numbers of 2.35 and 1.96 having different throat areas were used, thereby permitting two ranges of engine total-temperature rise ($\tau = 2$ and $\tau = 4$, respectively) without resulting in subcritical inlet operation. Both nozzles expanded the flow to the full engine diameter at the exit. Propylene oxide was utilized as a fuel.

The scavenge system included a 6.6-inch-diameter scoop mounted, as shown in figure 1, 3 inches downstream of the engine exit. A submerged spray coolant system (fig. 1) was located inside the scoop lip to lower the gas temperature in the vicinity of the scoop shell and thus prevent its possible structural failure and increase the total pressure of the exhaust jet. The scavenged gases were ducted through the tunnel side plate to the exhaust line as indicated in figure 1.

Pitot and static instrumentation were located throughout the engine and were used in determining engine operating conditions such as pressure recovery and nozzle static pressures. In addition, pitot and static rakes located in the tunnel exit and in the scavenge system were used to determine the operating pressure ratios. The jet-wake boundaries were surveyed with the temperature and humidity probes shown in figure 3. The humidity probe merely sampled the air, which was passed through a dew-point meter. A spike inlet was used on this probe to increase the pressure in the air-sampling circuit.

RESULTS AND DISCUSSION

Engine

The 30° half-angle single cone inlet of the ram-jet engine was designed for a mass-flow ratio of 0.76, which corresponded to a 9.7 percent capture of the tunnel flow. Stable subcritical operation was impossible with this inlet because of choking of the main stream; and, consequently, the investigation presented herein is for supercritical inlet operation with inlet-flow patterns of the type illustrated by the schlieren photograph in figure 4.

The combustion process was steady for both nozzle configurations ($\tau = 2$ and $\tau = 4$) up to the maximum values of fuel-air ratio used. The maximum fuel-air ratio for the $\tau = 2$ nozzle configuration was 0.04,

corresponding to a near-critical inlet condition and a combustion efficiency of 40 percent. The fuel-air-ratio limit for the $\tau = 4$ nozzle configuration was between 0.04 and 0.05, at which point thermal choking of the tunnel occurred at the nozzle exit. The combustion efficiency corresponding to this limiting condition was even less than the $\tau = 2$ nozzle efficiency. These low efficiencies indicate the probability of continued combustion downstream of the nozzle.

Exhaust Jet

A typical schlieren photograph of the $\tau = 2$ nozzle exhaust is presented in figure 5 for a fuel-air ratio of 0.017 with the scavenge system removed from the tunnel. As the fuel-air ratio increased, the exhaust-to-stream static-pressure ratio p_e/p_s (to be called hereinafter jet static-pressure ratio) increased, and the jet-wake widened. The Mach number of the external flow just upstream of the nozzle exit was determined to be approximately 2.2.

Quantitative measurements of the jet boundaries were obtained for a range of operating conditions from measurements of moisture and temperature. Typical humidity and temperature profiles are presented in figure 6. The humidity traverse plots indicate the limits of the moisture-contaminated jet. The temperature profiles indicate the extent of conduction and turbulent transport of heat. The jet boundary is defined by the radius at which the values of temperature and/or humidity reach a minimum. The jet boundaries as determined from a limited number of such surveys are summarized in the following table. Stations at 0.1- and 1.5-body diameters downstream of the nozzle exit are considered for several values of jet static-pressure ratio p_e/p_s which exert a direct influence on the jet spreading.

Jet static-pressure ratio, p_e/p_s	Jet boundary, y/r	Nozzle	Remarks
0.1 Diameter downstream of nozzle			
0.86	1.03	$\tau = 2$	Temperature survey
.95	1.02	$\tau = 2$	Humidity survey
1.00	1.11	$\tau = 4$	Temperature and humidity survey
1.5 Diameters downstream of nozzle			
0.84	1.25	$\tau = 2$	Temperature survey
.95	1.15	$\tau = 2$	Humidity survey
1.00	1.25	$\tau = 2$	Temperature survey
1.03	1.33	$\tau = 4$	Temperature survey

Of interest to the scavenge problem is the fact that the boundaries extended beyond the body diameter at only 0.1 diameter downstream even though the flow was overexpanded within the nozzle. This spreading may have resulted from the 2.5° divergence angle of the nozzle or from the turbulent transport of fluid into the boundary layer from the external engine surface.

Exhaust Scavenging

In figure 7 a sketch of the scavenge scoop selected for the present installation is shown superimposed on assumed linear variations of jet boundary between the two stations surveyed. The data show considerable scatter and it was necessary in some cases to estimate boundaries by joining points at different jet static-pressure ratios but, in general, they indicate the possibility of stream contamination in some cases with jet static-pressure ratios greater than 0.85.

The variation in jet static-pressure ratio with engine fuel-air ratio is shown in figure 8 for both the $\tau = 2$ and $\tau = 4$ nozzles. These data were obtained with the scavenge scoop in position and operating supercritically. All operating conditions yielding values of jet static-pressure ratio greater than approximately 0.8 to 0.84 resulted in contamination of the stream flow as measured with a humidity sampler, 5.6 scoop diameters downstream of the scavenge scoop. In a general way, then, these data confirm the predictions from the profile surveys. The $\tau = 2$ nozzle data points were obtained with supercritical operation of the scoop (fig. 9(a)), whereas the $\tau = 4$ points correspond to steady subcritical scoop operation (fig. 9(b)). Subcritical flow was usually present with the $\tau = 4$ configuration as an apparent result of the relatively low nozzle-exit Mach number, and continued combustion of the exhaust jet into the scavenge duct.

Reduction of the scavenge-system total-pressure ratio P_0/P_4 below the minimum operating values both contaminated the stream flow and influenced the pressures within the nozzle. High-speed motion-picture schlieren photography indicated that, in these cases, unsteady scoop operation was present with shock waves oscillating from within the scoop to within the nozzle. The effect increased as the scavenge system was further throttled.

Operating Pressure Ratios

Stagnation pressure ratios for the tunnel and scavenge-system operation are presented in table I. The subscripts refer to the stations indicated in figure 1.

Prediction of scavenge-system total-pressure ratios requires, in addition to a knowledge of engine characteristics, an evaluation of the piping losses and the effects of combustion of unburned fuel ahead of and within the scavenge system. An approximation of the piping losses has been made for the subcritical scoop ($f/a = 0$, see footnote d, table I). The piping losses from stations 3 to 4 are estimated to be 1.6q based on experimental pressures.

SUMMARY OF RESULTS

From an investigation of the scavenging of the exhaust of a 6-inch-diameter ram-jet engine in a Mach 3.1, 1- by 1-foot supersonic tunnel, the following results were obtained:

1. Scavenge scoop size can apparently be satisfactorily estimated from temperature and humidity surveys of the jet boundaries.
2. With a 6.6-inch-diameter scavenge system located 3 inches downstream of the engine exit, the exhaust gas was successfully scavenged for jet static-pressure ratios up to 0.85.
3. Reduction of scavenge-system total-pressure ratio by throttling beyond some critical value resulted in unsteady operation with the scavenge-scoop shock wave oscillating from within the scoop to within the engine exhaust nozzle.

Lewis Flight Propulsion Laboratory
National Advisory Committee for Aeronautics
Cleveland, Ohio, November 29, 1954

3158

TABLE I. - OPERATING PRESSURE RATIOS

Item	Experimental pressure ratios		Normal shock calculation
	P_0/P_5	P_0/P_4	
Empty tunnel performance			
Starting ^a	4.1		3.38
Operating ^b	4.0		3.38
Tunnel performance with engine and scavenge system installed			
Tunnel starting:			
$f/a = 0$; scoop supercritical	4.46		4.43 ^c
Tunnel operating:			
$f/a = 0$; scoop supercritical	4.18		
$f/a = 0.04$; $\tau = 2$ engine and scoop supercritical	4.35		
Scavenge-system performance for no tunnel contamination			
Supercritical scoop:			
$f/a = 0$; no coolant		8.19	
$f/a = 0$; coolant		10.49	
$f/a = 0.039$; $\tau = 2$ engine; small coolant		5.43	
$f/a = 0.04$; $\tau = 2$ engine; increased coolant		5.70	
$f/a = 0.04$; $\tau = 2$ engine; no coolant		7.83	
Subcritical scoop:			
$f/a = 0$; no coolant		9.27 ^d	6.52

^aInitially establishing supersonic flow throughout test section.

^bMinimum pressure ratio which may be realized with supersonic flow maintained throughout test-section areas.

^cExperimental values of scoop inlet Mach number and P_0/P_3 were used in this calculation.

^dPiping losses were calculated from this point for system.

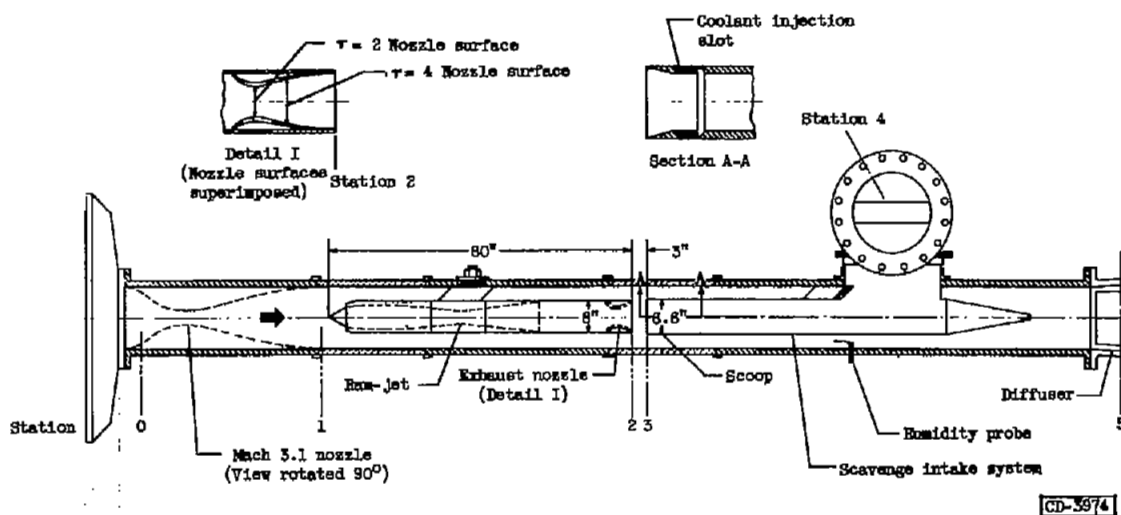
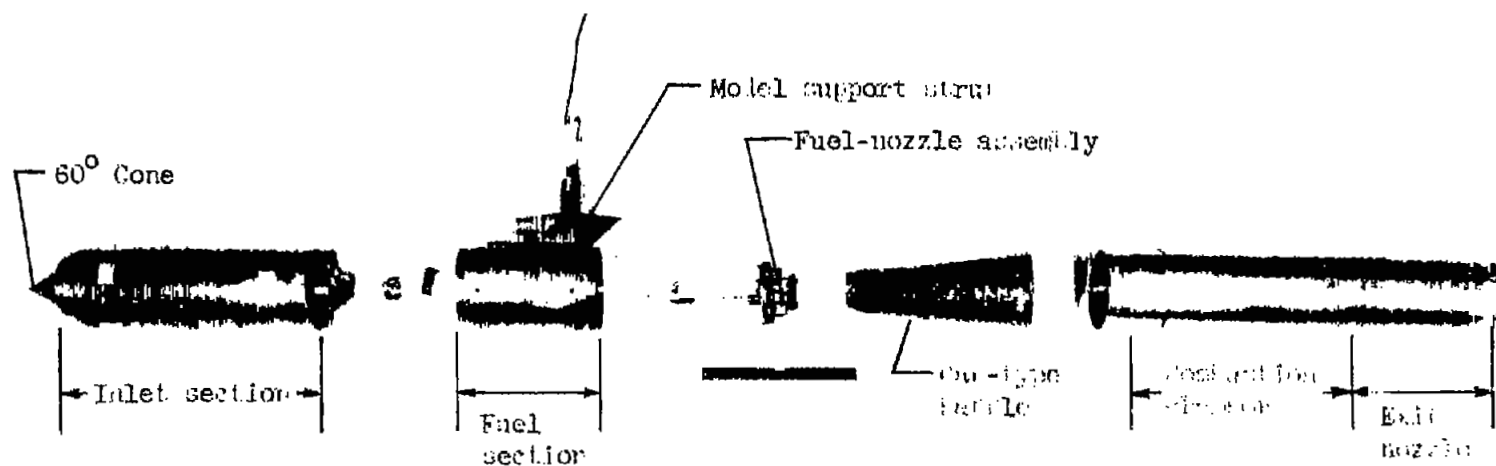


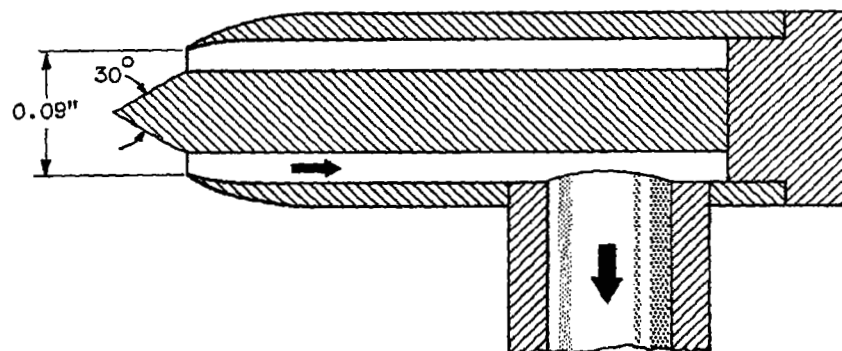
Figure 1. - Ram-jet engine and scavenge-system installation.

$\tau = 2$		$\tau = 4$	
Distance upstream of nozzle exit, x, in.	Radial distance from nozzle axis, y, in.	Distance upstream of nozzle exit, x, in.	Radial distance from nozzle axis, y, in.
0	2.900	0	2.900
2.25	2.800	2.25	2.800
2.75	2.760	2.75	2.768
3.25	2.705	3.25	2.730
3.75	2.640	3.75	2.688
4.25	2.520	4.25	2.638
4.75	2.500	4.75	2.530
5.25	2.420	5.25	2.520
5.75	2.340	5.75	2.455
6.25	2.252	6.25	2.382
6.75	2.160	6.75	2.310
7.25	2.065	7.00	2.270
7.75	1.960	7.25	2.275
8.00	1.915	7.75	2.275
8.25	1.820	8.25	2.290
8.75	2.000	8.75	2.320
9.25	2.160	9.25	2.367
9.75	2.410	9.75	2.472
10.16	2.680	10.16	2.690

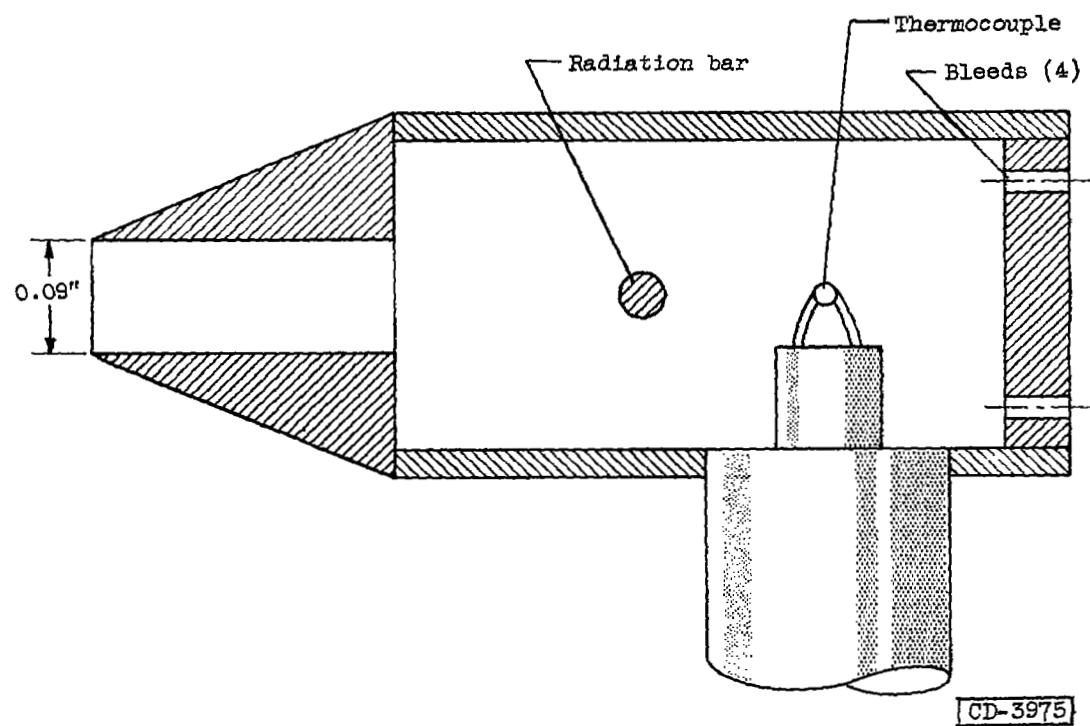


C-30748

Figure 2. - Components of 6-inch-diameter ram-jet engine.



(a) Humidity probe; X5.



(b) Aspirating thermocouple; X5.

Figure 3. - Instruments used in exhaust-jet survey.

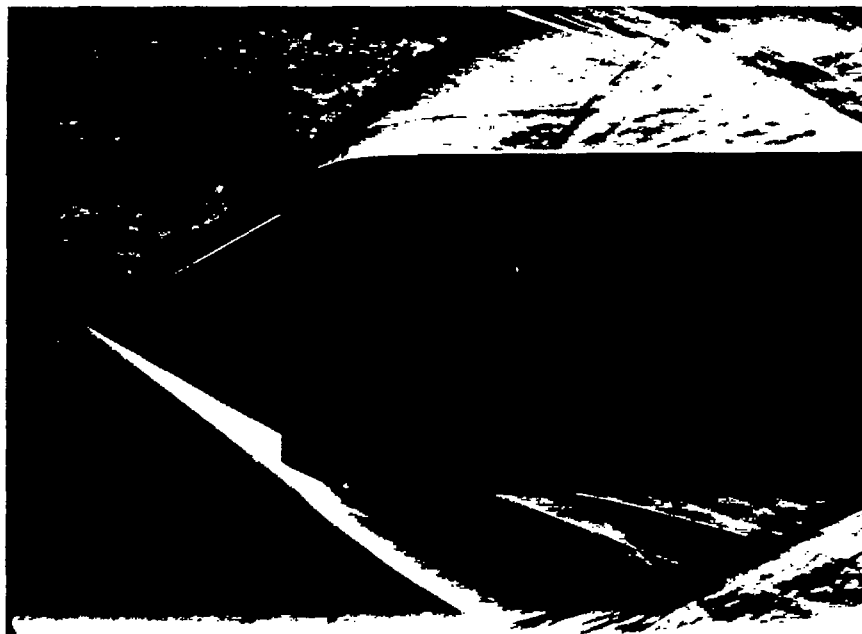


Figure 4. - Schlieren photograph showing inlet-flow pattern.

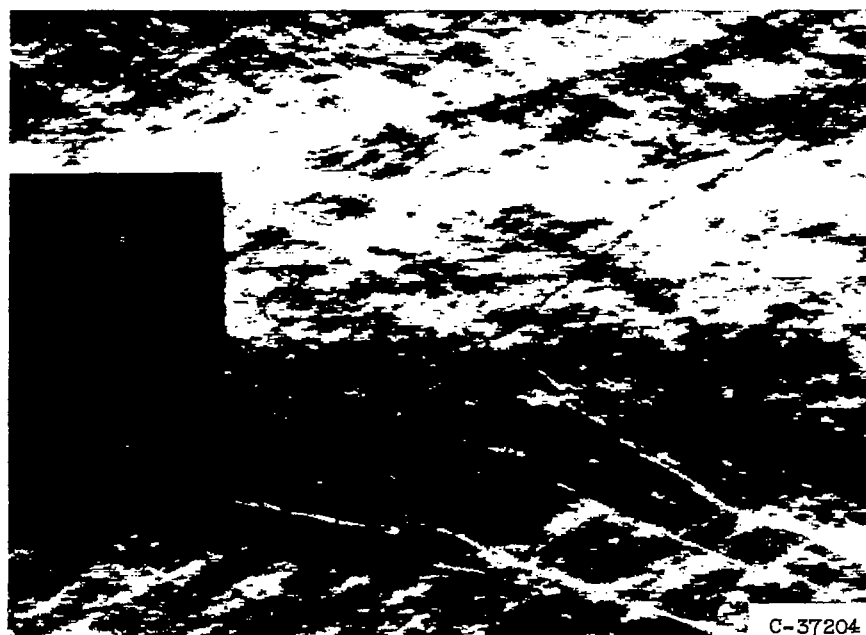
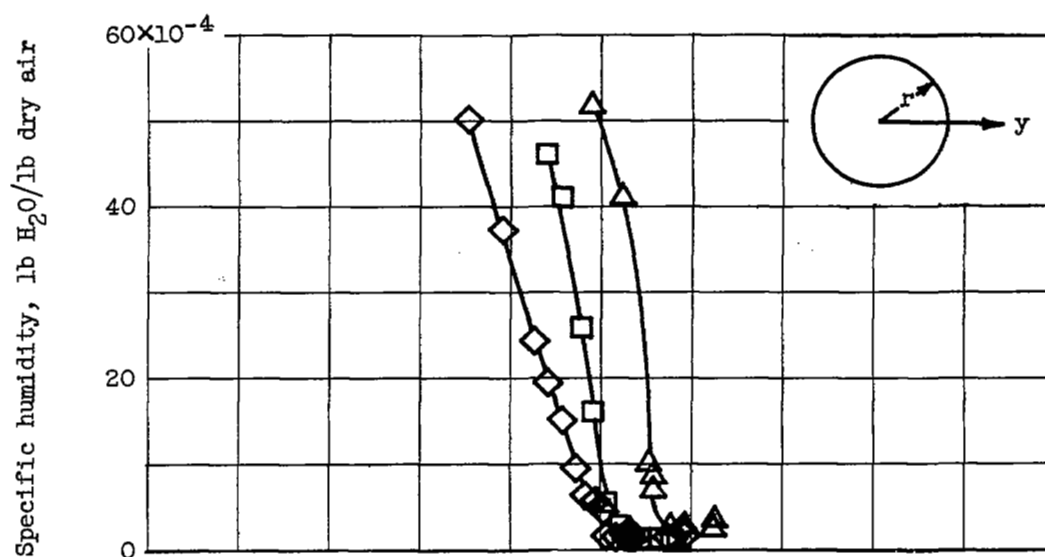


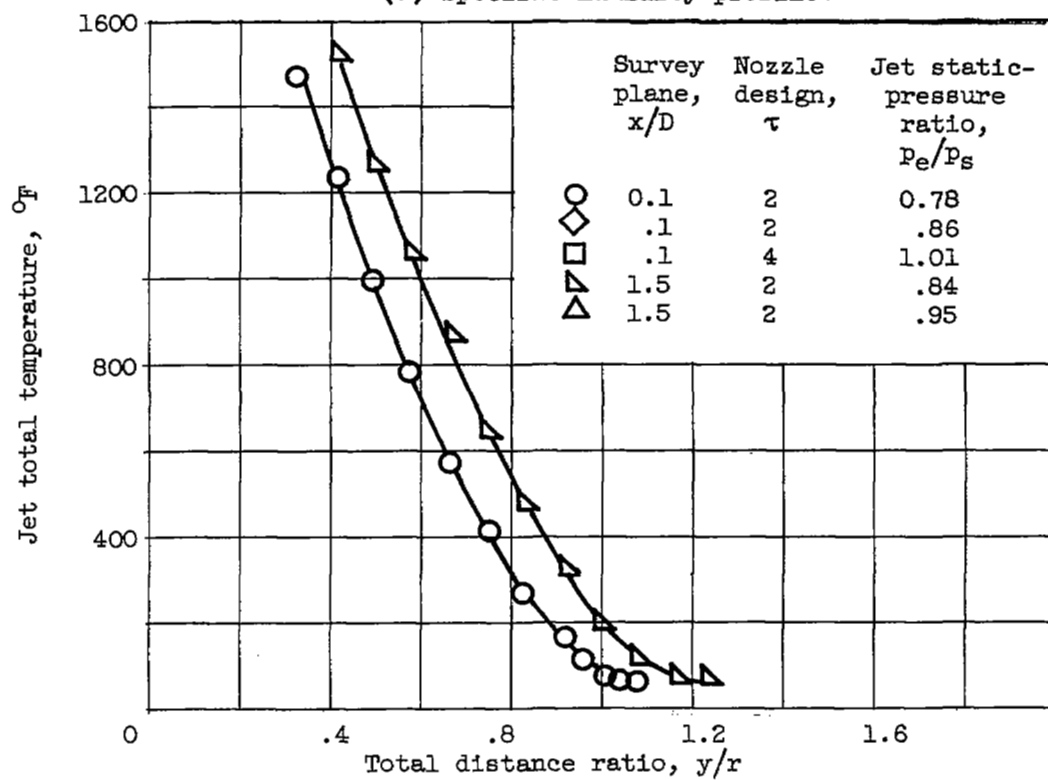
Figure 5. - Schlieren photograph of exhaust jet. Fuel-air ratio, 0.017; jet static-pressure ratio, 0.56.

3158

CH-2 back



(a) Specific humidity profile.



(b) Total-temperature profile.

Figure 6. - Typical exhaust-jet profiles.

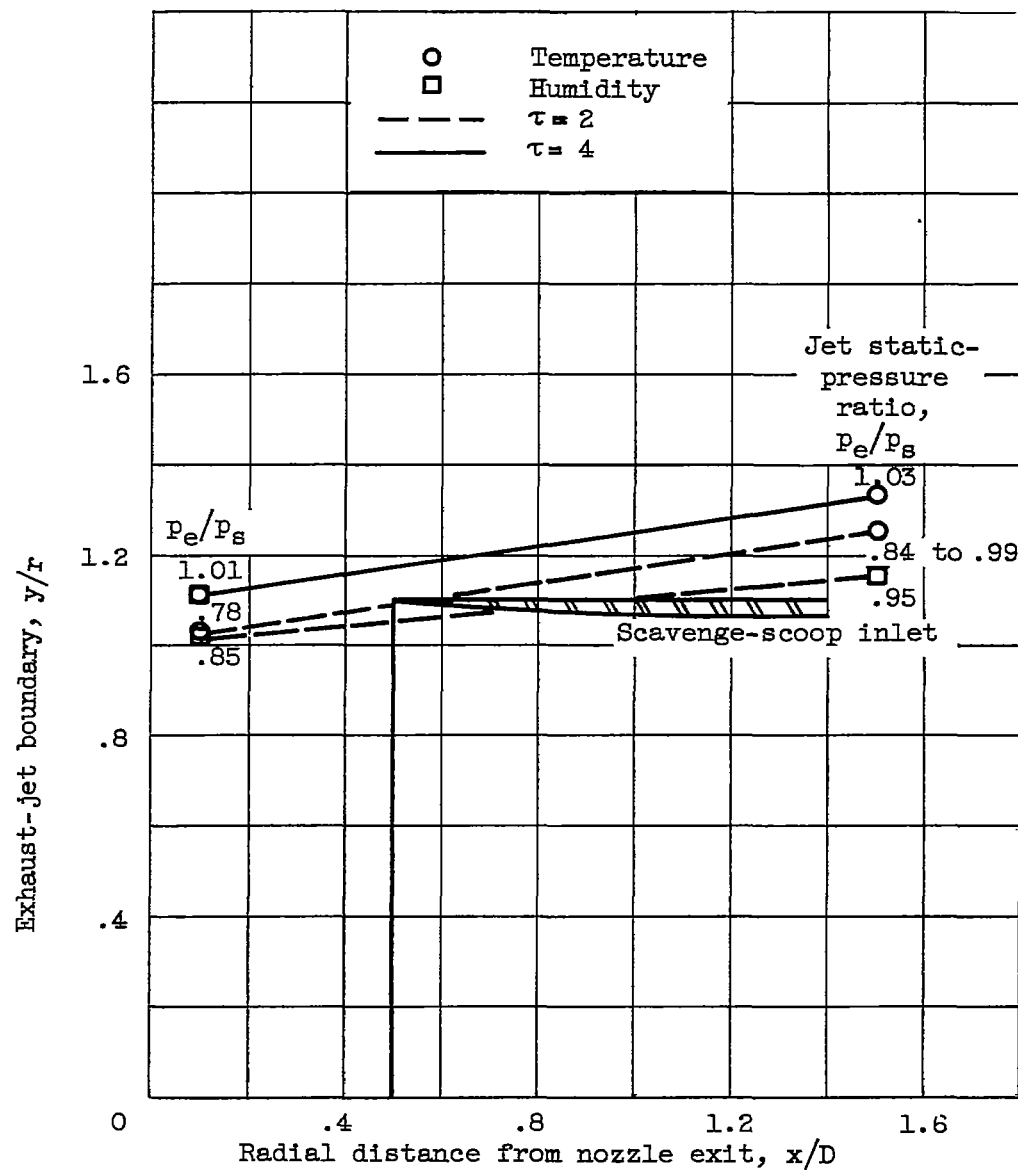


Figure 7. - Exhaust-jet spreading.

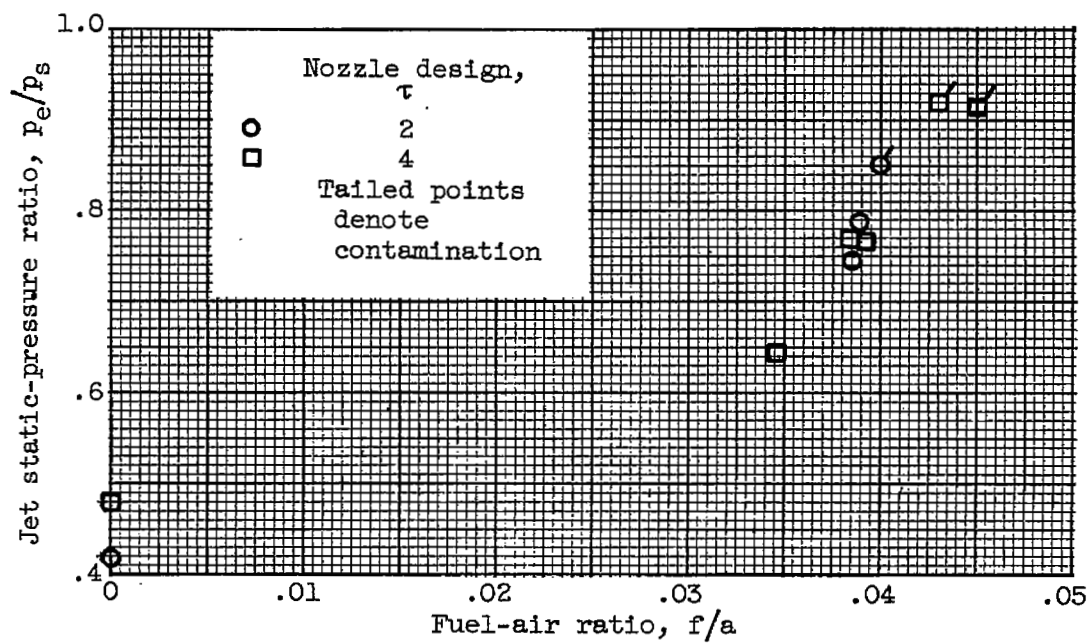
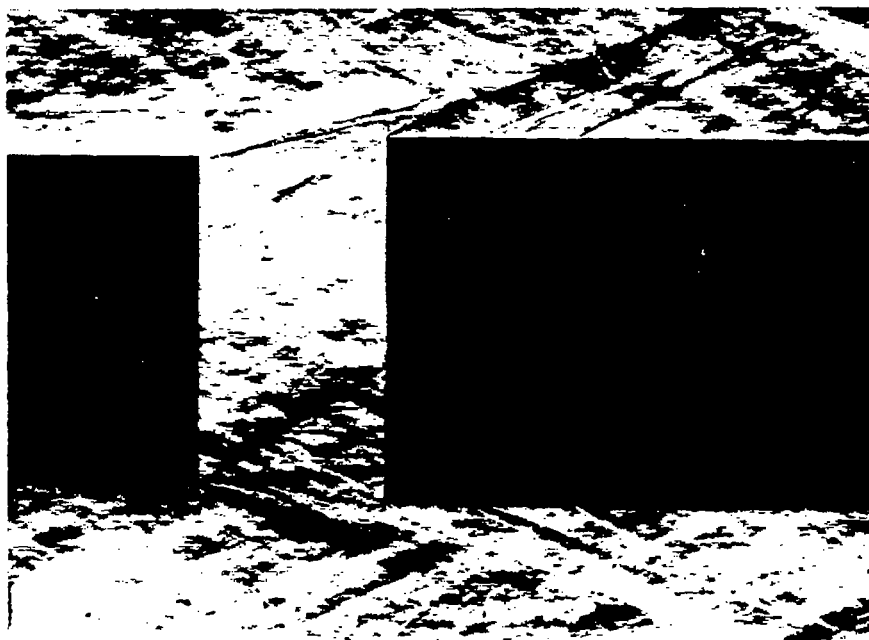
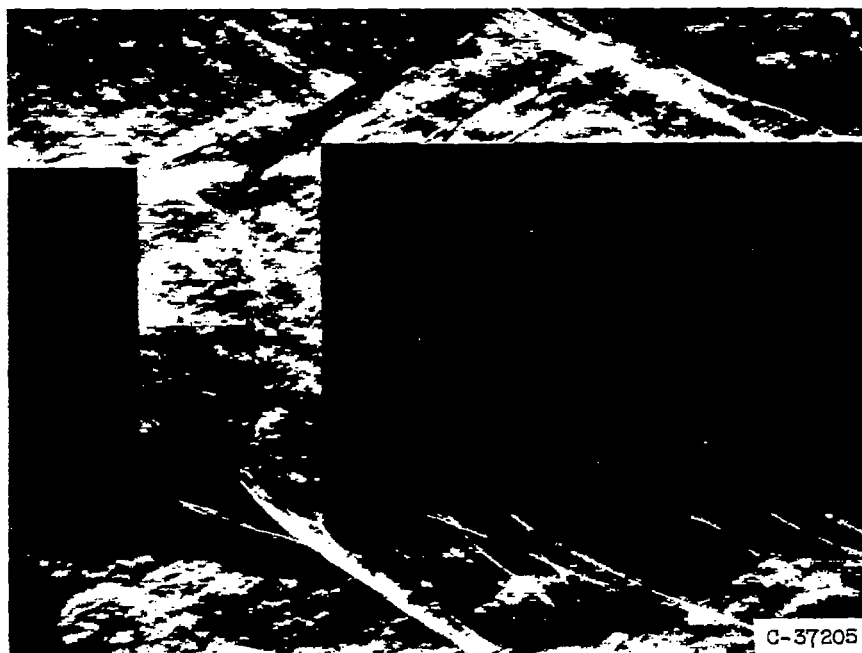


Figure 8. - Scavenge effectiveness.



(a) Supercritical scoop operation of $\tau = 2$ nozzle configuration.



(b) Subcritical scoop operation of $\tau = 4$ nozzle configuration.

Figure 9. - Schlieren photographs of exhaust jet into scavenge inlet showing supercritical and subcritical scoop operation.



3 1176 01435 7694

1. The first part of the document is a review of the literature on the subject of the effect of the environment on the behavior of the human operator.

2. The second part of the document is a review of the literature on the subject of the effect of the environment on the behavior of the human operator.

3. The third part of the document is a review of the literature on the subject of the effect of the environment on the behavior of the human operator.